ELSEVIER

# Water clusters studied by electrospray mass spectrometry

Gustaf Hulthe[a], Gunnar Stenhagen[b,*], Olof Wennerström[b], Carl-Henrik Ottosson[b]

[a]*Department of Analytical and Marine Chemistry, University of Göteborg, S-41296 Göteborg, Sweden*
[b]*Department of Organic Chemistry, Chalmers University of Technology, S-41296 Göteborg, Sweden*

## Abstract

By a slight modification of the electrospray ionization method, positively charged water clusters $H^+(H_2O)_n$ can conveniently be studied by high-resolution mass spectrometry over a large range of masses (from 1 to well over 100 water molecules). Inclusion of an ammonium ion instead of a hydronium ion in the clusters does not lead to a change in the distribution, and this indicates similar structures for the two types of clusters. In small ammonia–water clusters the frequency of ammonia is higher than predicted by statistics, whereas the opposite is true for large ammonia–water clusters. Similarities in the distribution of clusters generated from pure water and from an ammonia–water mixture gives doubt about proton delocalization on the cage surface. Instead, structures which have a central hydronium or ammonium ion are more likely. A new suggestion is made about structures of the well-known clusters $H_3O^+(H_2O)_{20}$ and $NH_4^+(H_2O)_{20}$.    © 1997 Elsevier Science B.V.

*Keywords:* Water clusters; Cations; Hydronium ion; Ammonium ion

## 1. Introduction

Small ions such as the hydronium ion ($H_3O^+$) and the ammonium ion ($NH_4^+$) can exist hydrogen-bonded to a number of water molecules in clusters even in gas phase. This has been confirmed experimentally by a large number of investigations (for reviews on cluster ions, see, e.g., [1,2]). Ions with a certain number of water molecules are more stable and more frequent than others, and there has been a particular interest in ions that consist of twenty water molecules surrounding the hydronium or ammonium ion [3–16]. In this regard, one should note that the number twenty is also the number of corners in one of the classical regular polyhedra, the dodecahedron. Therefore, structures of the ions mentioned above has often been discussed in terms of a shell of water molecules in the form of a more or less distorted dodecahedron surrounding a hydronium or ammonium ion.

We now report a facile method to study such water clusters containing positive ions by high-resolution mass spectrometry (resolution >5000 with 10% valley def.) using a slightly modified electrospray inlet system. In all earlier experiments it is clear that the clusters have been formed from free vapor water molecules at low temperatures and high velocity/ shearforces (i.e. supersonic conditions). Using electrospray it is likely that the clusters arise, contrary to previous methods, from already mono-charged, larger packets of water molecules evaporating in vacuum while losing energy, until they reach equilibrium and Boltzmann distribution. Multiply charged droplets can split electrostatically so that singly charged units are formed. During the short time of flight from the inlet into vacuum and the start of mass separation we assume that the cluster reaches equilibrium thermodynamically. Much larger

cluster distributions are observed with this technique, and this indicates that our new method utilizes lower temperatures and energies than previous methods [3–16], which instead have been based on, for example, electron impact ionization.

## 2. Experimental

A ZabSpec double focusing magnetic sector mass spectrometer equipped with an hexapole lens electrospray interface (VG Analytical, Fisons Instruments, UK) was used in our studies. For water cluster ions, the conditions of the atmospheric part of the interface were slightly changed: i.e., no bath gas flow, no heating of the spray chamber (making it cooler than 20°C), and a higher velocity in combination with lower mass flow (20 l/h at atmospheric pressure) of the nebulizing gas. The latter was achieved by high gas pressure (15 bar of nitrogen) and a narrow gap between the outlet tip of the capillary tube and the outer tube making the nebulizer gas pressure and temperature drop rapidly inside the interface. Fig. 1 shows a schematic diagram of the interface.

The liquid flow was 30 μl/min using a syringe pump, Phoenix 20 (Carlo Erba, Fisons Instruments, Italy). A 500 μl loop injector (Reodyne 2840) was used for sample injections. To avoid electrical discharge in the feeding capillary and in the pumping line the ion concentration of the test solution, which governs the conductivity, was limited to less than 100 m$M$. This experimental set-up made it very easy to obtain high-quality cluster spectra on a number of different solutions.

## 3. Results

In previous methods, used to generate water cluster ions [3–17], a mixture of water vapor and carrier gas was expanded adiabatically and supersonically into high vacuum. Corona discharge [4,5], electron impact [7,9], as well as laser beam or UV photoionization [8,10,11,15,16], and thermospray [17] have been utilized to achieve cluster ions. In some of these set-ups it was necessary to use a cold inlet channel.

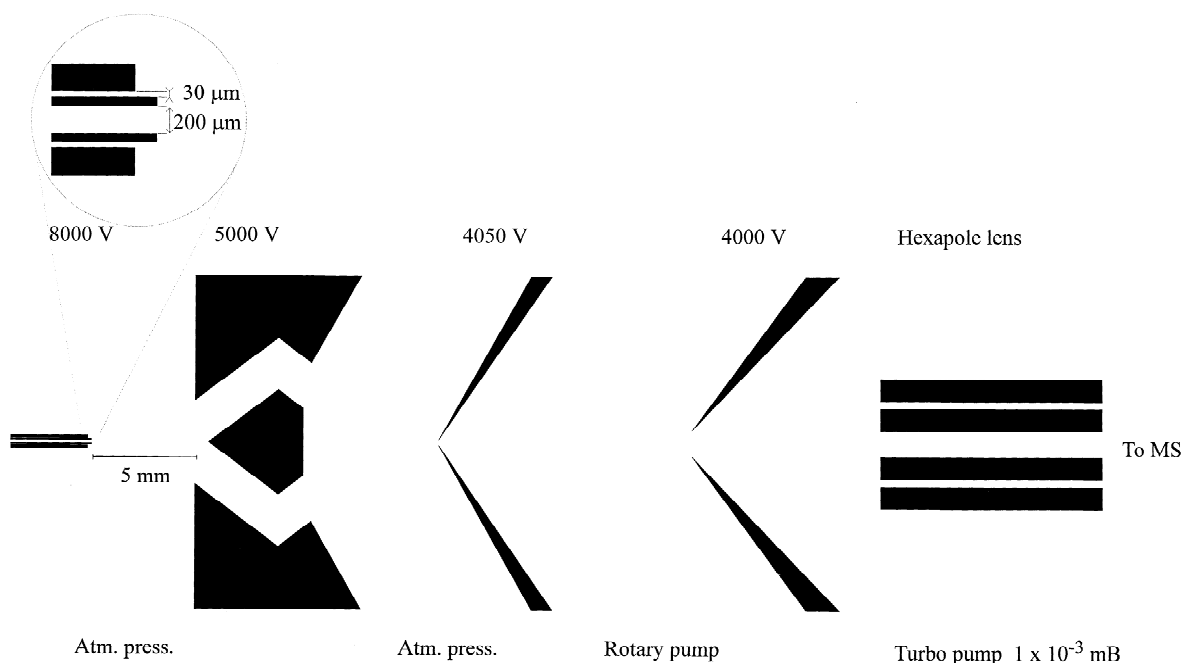In the electrospray ionization chamber, liquid and



Fig. 1. Schematic diagram of the modified electrospray inlet system.

gas are mixed under adiabatic expansion conditions so that charged droplets or particles are given. These are reduced in size until cluster ions are formed.

To optimize the cluster ion production at least five properties of the nebulizing gas have to be considered, namely;

1. Its cooling effect while expanding.
2. The ability of the gas molecule to become ionized and transfer an electron so that a charged cluster is formed.
3. The ability of the gas to serve as a reagent in associative and in de-excitation collision processes that effect the cluster ion size distribution [5].
4. The d.c.-plasma susceptibility as there are steep potential ramps in the ion source.
5. The ability of the gas to form hydrogen bonds.

Five different gases were tested: helium, carbon dioxide, nitrogen, oxygen and argon. Normally, electrospray is run with nitrogen as the nebulizing

gas. Of the other gases, helium did not work because of problems associated with maintaining a good vacuum, carbon dioxide worked similar to nitrogen, and oxygen gave weak signals and more complex spectra. For the larger clusters up to a hundred times higher signals were achieved with argon compared to nitrogen; however, it sometimes caused electrical discharge in the pumping line. Previously, it was observed that argon ions do contribute to the formation of larger water clusters [5]. Therefore, a mixture of nitrogen and argon could be optimal, but we used nitrogen as the nebulizing gas in most of the experiments.

A high-resolution mass spectrum of $H_3O^+(H_2O)_n$ with $3<n<120$ is shown in Fig. 2A. The ion with mass $m/z=73$ is the base peak, and corresponds to the $H_3O^+(H_2O)_3$ cluster ion, previously thoroughly investigated [18–26]. It should be noted that the maximum peak sometimes appears also at the ion with $m/z=55$. Whether the maximum is located at
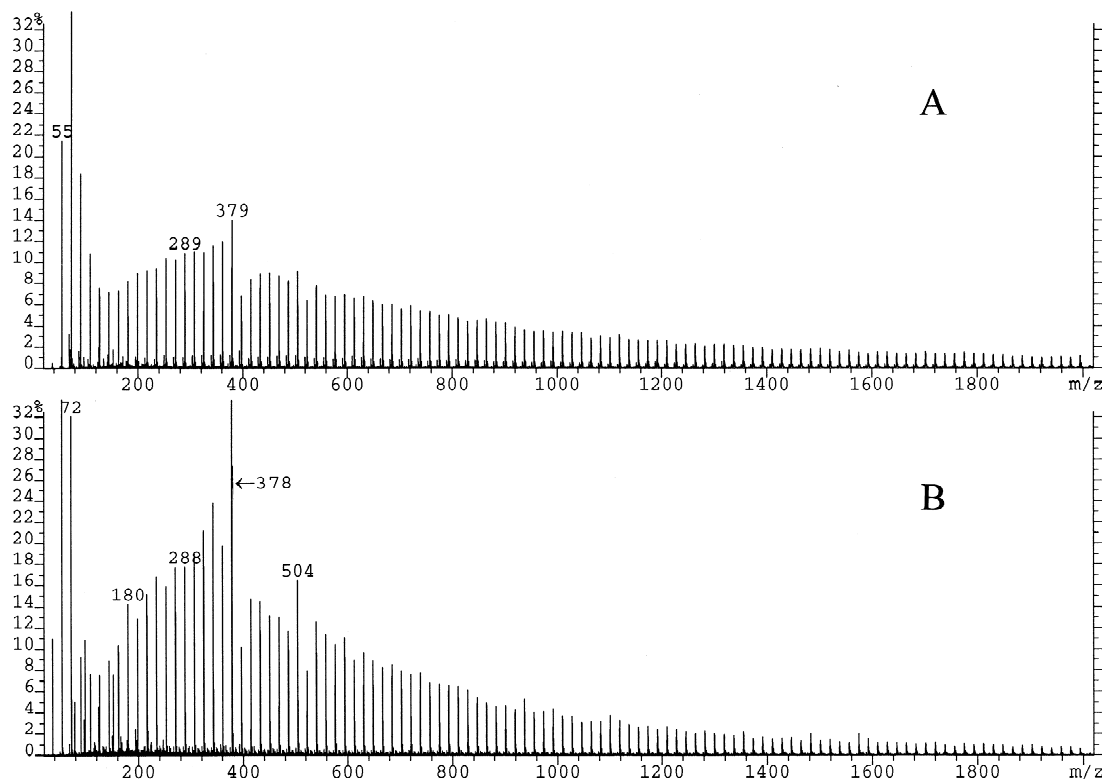


Fig. 2. High resolution mass spectrum of positively charged water clusters. Spectrum A is pure water and B is water with 0.5% $NH_3$.

$m/z=55$ or 73 depends on the setting of the inlet system, and is most likely due to the temperature in the inlet channel.

After the maximum at $H_3O^+(H_2O)_3$ the intensity declines and reaches a minimum at $H_3O^+(H_2O)_8$, and then slowly increases again. A second maximum is reached at $m/z=379$, corresponding to the well-known $H_3O^+(H_2O)_{20}$ cluster ion [3–16]. Finally, a third and smaller bump in the intensity corresponds to the $H_3O^+(H_2O)_{27}$ cluster ion. Thereafter, the intensities fall off slowly but there are also clusters at $m/z=2000$, e.g. $H_3O^+(H_2O)_{120}$, which give significant peaks, and there are no difficulties in obtaining a high resolution also at these high mass numbers. If ammonia or an ammonium salt at concentrations of 10 $\mu M$–10 m$M$ is added to water then the positive charge is located on the ammonium ion. Clusters that contain one and only one ammonium ion are seen in the spectrum shown in Fig. 2B, and the peaks appear at one mass unit lower than those of the corresponding water clusters in Fig. 2A.

Mixed ammonium–water clusters were investigated in more detail and the concentration of ammonia in the sample solutions was varied from 0.5 to 33%. Thereby, an increasing number of ammonia molecules are allowed to incorporate into the cluster ions. Details from the spectra on samples containing 0.5%, 12.5% and 33% $NH_3$, and an analysis of the $NH_3$ content in these clusters, are shown in Figs. 3–5. The peaks of protonated clusters composed of 80 water or ammonia molecules are expanded in Fig. 3. Thus, the high resolution is clearly seen. Insert A shows the measured spectra, while inserts B–E show calculated mass compositions from the natural content of $^{18}O$ and $^2H$ in $NH_4^+(H_2O)_{79}$ to $NH_4^+(NH_3)_3(H_2O)_{76}$.

The magic number of twenty is valid only for the number of water molecules, and not for the total number of molecules surrounding the central ion. In this regard, the phrase 'magic' refers to a cluster ion with a higher relative abundance than those of comparable sizes. In Fig. 5 it is seen that $NH_4^+(NH_3)_4(H_2O)_n$ reaches a maximum at a total of 10–13 units, whereas $NH_4^+(NH_3)_3(H_2O)_n$ is most frequent at 12–16 units. Clusters that contain less ammonia reach maxima at sites corresponding to $NH_4^+(H_2O)_{20}+nNH_3$ where $n$ is either 1 or 2. A strong peak is also reached for the cluster

$NH_4^+(H_2O)_{20}(NH_3)_3$ and it seems as if ammonia would coordinate to an already existing $NH_4^+(H_2O)_{20}$ clathrate structure. This gives the idea that large clusters are more like ice and prefer water while small clusters earn energy by adding ammonia.

Finally, clusters generated from water samples containing either hydrazine, hydrogenperoxide or hydroxylamine were analysed, as seen in Fig. 6.

## 4. Discussion

As observed in Fig. 2A, the $H_3O^+(H_2O)_3$ cluster ion is the base peak for protonated water clusters, and this ion has previously been investigated experimentally as well as theoretically [18–26]. Thereby, it was concluded to have a $C_3$-symmetric structure with a central hydronium ion hydrogen-bonded to three equally positioned $H_2O$ molecules [24–26]. Wei and Salahub investigated slightly larger protonated clusters up to $H_3O^+(H_2O)_5$ with DFT (Density Functional Theory) quantum chemical methods [26] (for recent reviews of DFT methods in computational chemistry see, e.g., [27]), and found that $H_3O^+$ is the central unit in all of the lowest energy structures.

Among the first to propose a structure for the $H_3O^+(H_2O)_{20}$ ion was Kassner and Hagen, when a dodecahedron $(H_2O)_{20}$ with a hydronium ion $H_3O^+$ in the interior of the cavity was suggested [4]. However, there were also suggestions that the proton resides on the surface of the dodecahedron and that it rapidly jumps between different O atoms [12]. Magnera et al. [13] found that the energy for the loss of $H_2O$ is larger for $n=20$ than for $n=19$ or 21, and that the stability of large clusters is due to enhanced possibilities for hydrogen bonding and not to electrostatic interactions. However, Shi et al. [16] in opposition stated that entropic rather than energetic effects give rise to the appearance of magic numbers.

In addition to experimental data, recent quantum chemical investigations gave various suggestions about the structure of the $H_3O^+(H_2O)_{20}$ cluster ion [28,29]. According to the semiempirical ZINDO calculations performed by Khan, the proton is located on the surface of a distorted dodecahedron $H^+(H_2O)_{20}$ and one $H_2O$ molecule is enclosed in the central cavity [28]. It was proposed that the magic appearance of the cluster at $n=20$ is due to a high
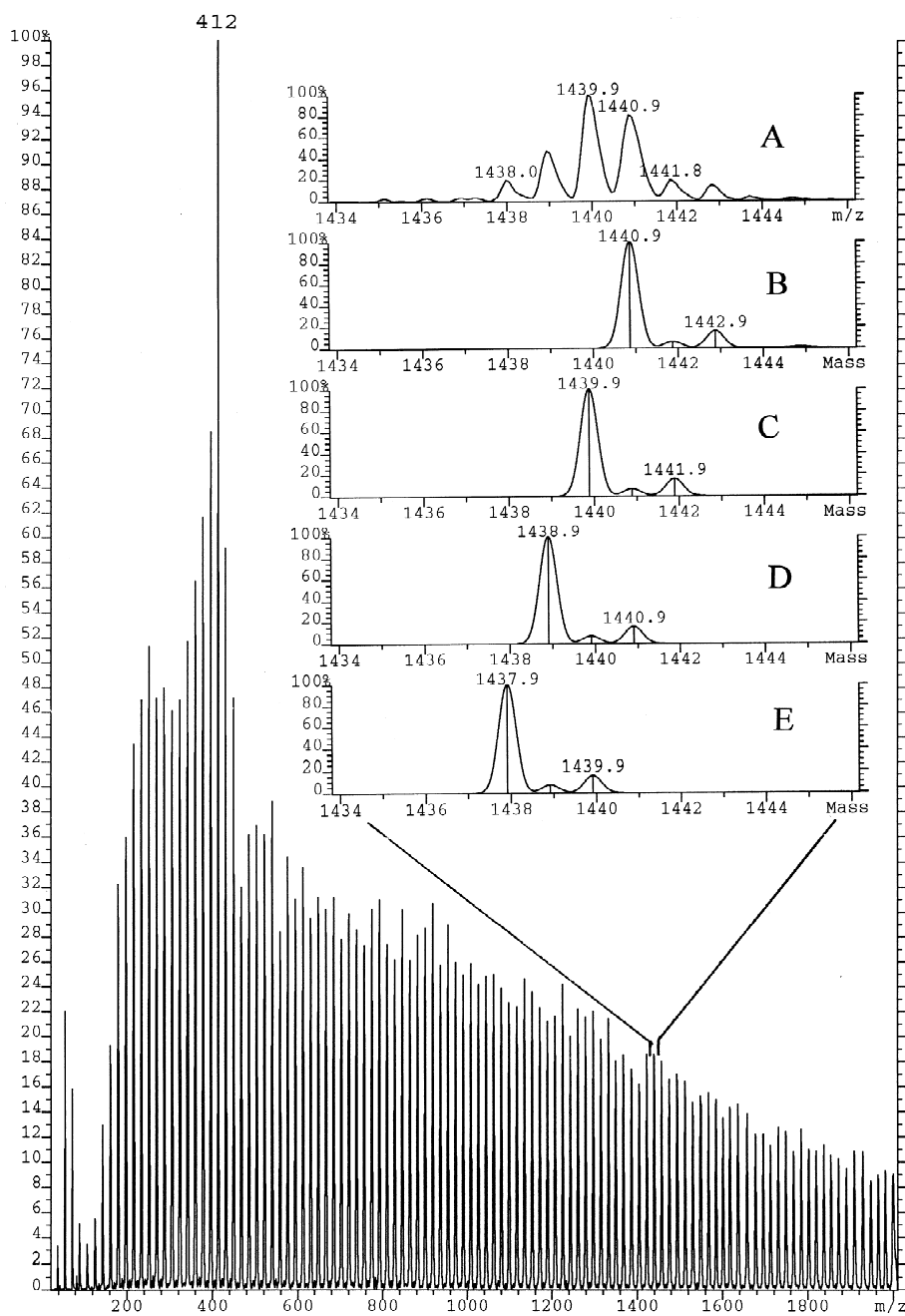
Fig. 3. High-resolution mass spectrum of positively charged ammonia–water clusters (33% NH$_3$). Insert in figure: expanded 1440 $m/z$ region (A) and isotope intensity simulation of ion composition with one (B), two (C), three (D) and four (E) ammonia/ammonium species.

stability of H$_3$O$^+$(H$_2$O)$_{19}$ instead of H$_3$O$^+$(H$_2$O)$_{20}$, and that the latter ion is formed since there is a high possibility for capture of a H$_2$O molecule when the clathrate structure is formed. However, according to DFT calculations by Laasonen and Klein there are instead several low-energy structures of
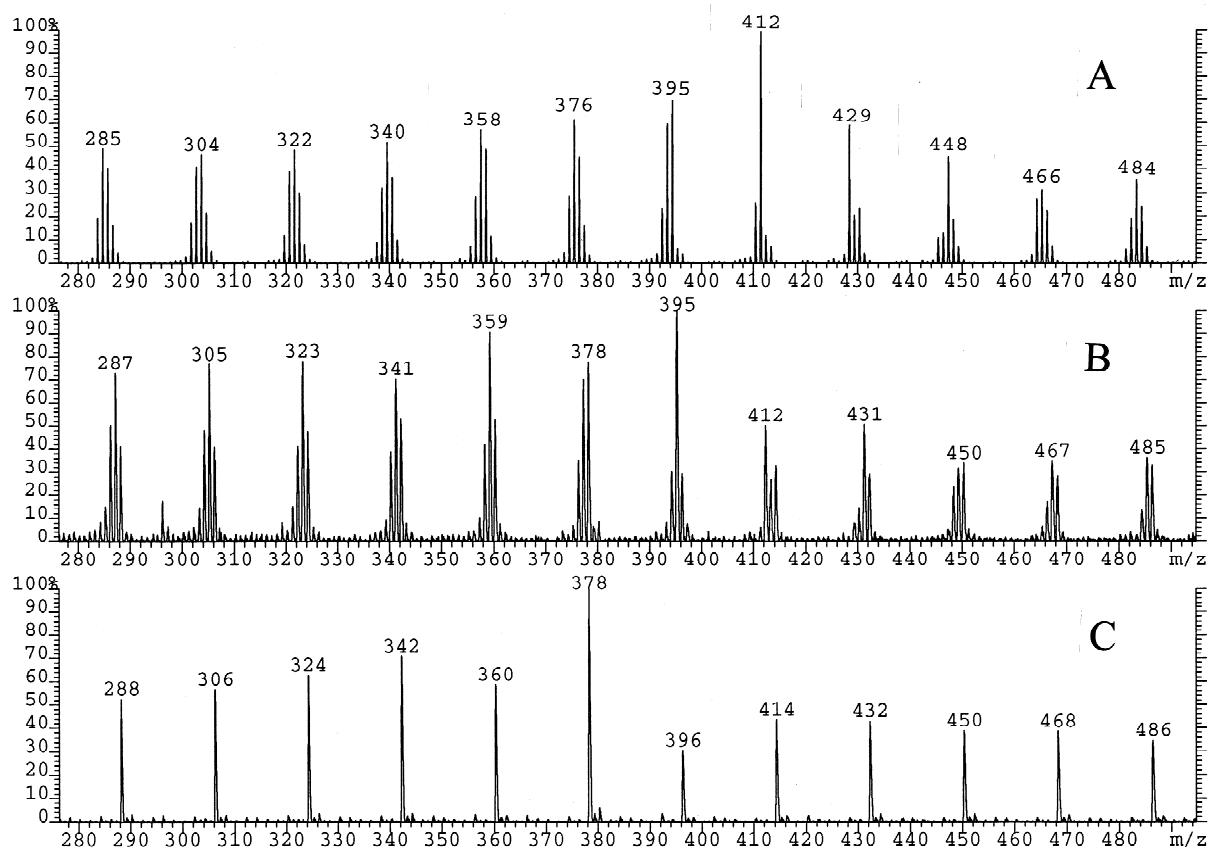
Fig. 4. Selective parts of mass spectra of positively charged ammonia–water clusters with three different ammonia concentrations: (A) 33%, (B) 12.5% and (C) 0.5%. The ammonia–water clusters at low concentration (C; 0.5%) contain one and only one ammonia with masses one unit less than the corresponding water clusters.

$H_3O^+(H_2O)_{20}$ that are within 1 kcal/mol in stability of each other [29]. Of these, two were distorted dodecahedral structures with the hydronium ion located close to the cage surface.

The structures of very large $H_3O^+(H_2O)_n$ cluster ions should asymptotically approach the ice structure of the bulk. Since there is no clear tendency for magic numbers in clusters with $n>30$ (Fig. 2A and B), it seems as if the passing from well-defined structures to bulk structures occurs in clusters with 20–30 water molecules.

Because of the similarity in the spectra of $H_3O^+(H_2O)_n$ and $NH_4^+(H_2O)_n$ cluster ions it is obvious that the two types of clusters are built in the same way, i.e. with $NH_4^+$ simply replacing $H_3O^+$. Another investigation of this type was previously undertaken by Shinohara et al. [8]. The similarity of

the spectra in Fig. 2A and B is an indication that a structure of $H_3O^+(H_2O)_{20}$ with a non-classical $H_5O_2^+$ unit located on the surface of a dodecahedron, such as that proposed by semiempirical calculations [28], should be questioned since structures with a bridged proton are not formed between $NH_4^+$ and $H_2O$. It has been found by quantum chemical calculations that proton jumps do not occur between $NH_4^+$ and $H_2O$, and a hypothetical structure with the proton on the O atom instead of the N atom is as much as 25 kcal/mol higher in energy at the MP4 level of theory [30] (1 cal=4.184 J). The structure of $NH_4^+(H_2O)$ should be compared with the bridged structure of $H_5O_2^+$ where the proton is symmetrically situated between the O atoms at H–O distances of 1.195 Å [31].

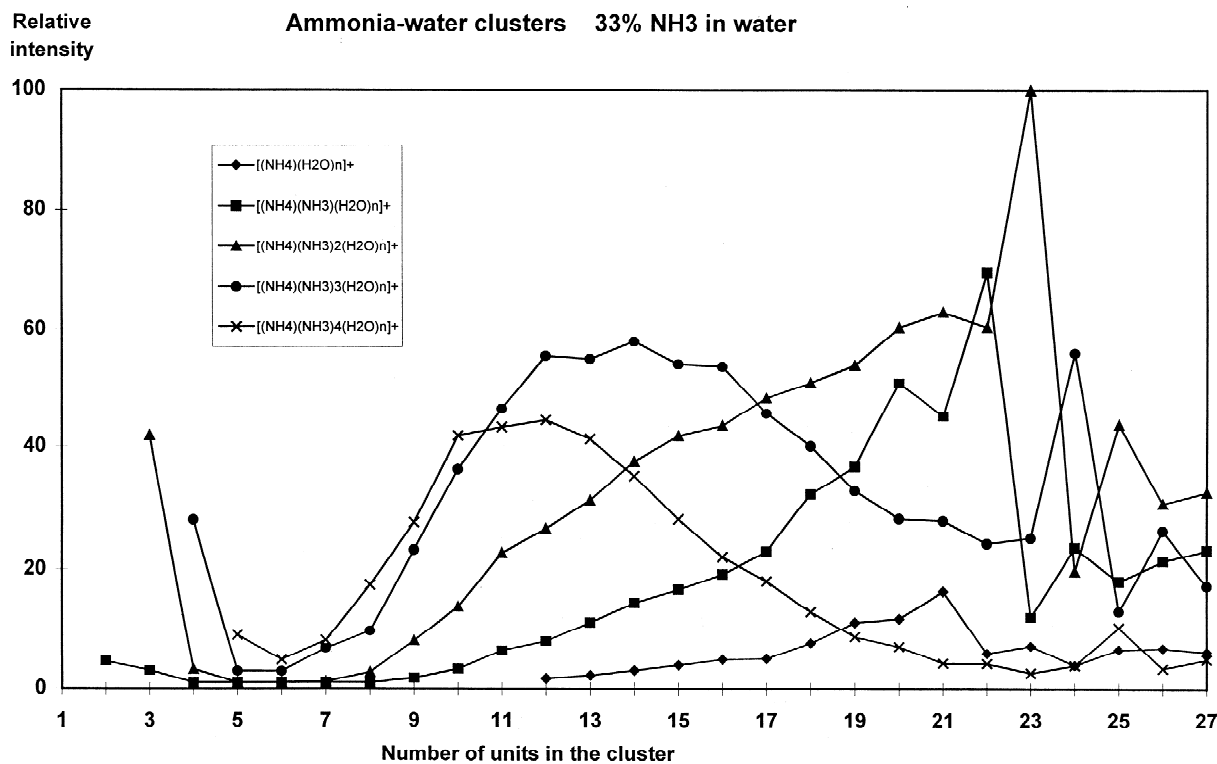Analysis of clusters obtained from the solutions

Fig. 5. A representation of relative intensities of $NH_4^+(NH_3)_n(H_2O)_m$ homologs with fixed $n$.

with various ammonia content reveals that ammonia is not statistically distributed in the different clusters. It is clearly more frequent in small clusters and less frequent in large clusters than in the original solutions. In clusters with the total number of heavy atoms being roughly 20, the distribution of ammonia is lower than expected. For example, it is seen in Fig. 4C that the largest peak in 33% ammonia is centered at $m/z=412$, corresponding to $NH_4^+(NH_3)_2(H_2O)_{20}$. This cluster ion therefore contains merely 13% $NH_3/NH_4^+$ and not the anticipated 33%. The ammonia content in slightly smaller clusters with 16–22 heavy atoms is at most 25%, but rises in smaller clusters to finally end at 100% for clusters composed of 2–5 units.

The spectra of these ammonium–water clusters can be rationalized by a few concepts: When $NH_4^+$ has only one ligand (I), it is best stabilized by ammonia instead of water. With two ligands (II), two ammonia molecules are preferred rather than one ammonia and one water molecule. With three ligands (III) the best combination is three ammonia rather than two ammonia and one water molecule. This rule of thumb is supported by quantum chemical DFT calculations performed at the B3LYP/6-311+G(d,p) level ( [32,33]; calculations were performed with the quantum chemical program package Gaussian94, Revision C.3 [34]) on cluster ions containing one central ammonium ion and 1–3 ammonia or water ligands (Fig. 7). Total coordination energies for these small clusters, as well as H–N and H–O hydrogen bond lengths, are given in Table 1. It can be seen that replacing a $H_2O$ with a $NH_3$ molecule leads to an increase in the coordination energy by 2.8–6.3 kcal/mol. The higher coordination energy of $NH_3$ compared to $H_2O$ should be due to different donicities (DN($NH_3$)=59 kcal/mol and DN($H_2O$)= 33 kcal/mol) [35], which leads to stronger hydrogen bonds for ammonia.

However, when the number of ligands increases further and when the ligands can form a ring or take part in hydrogen bonding to a second shell of water
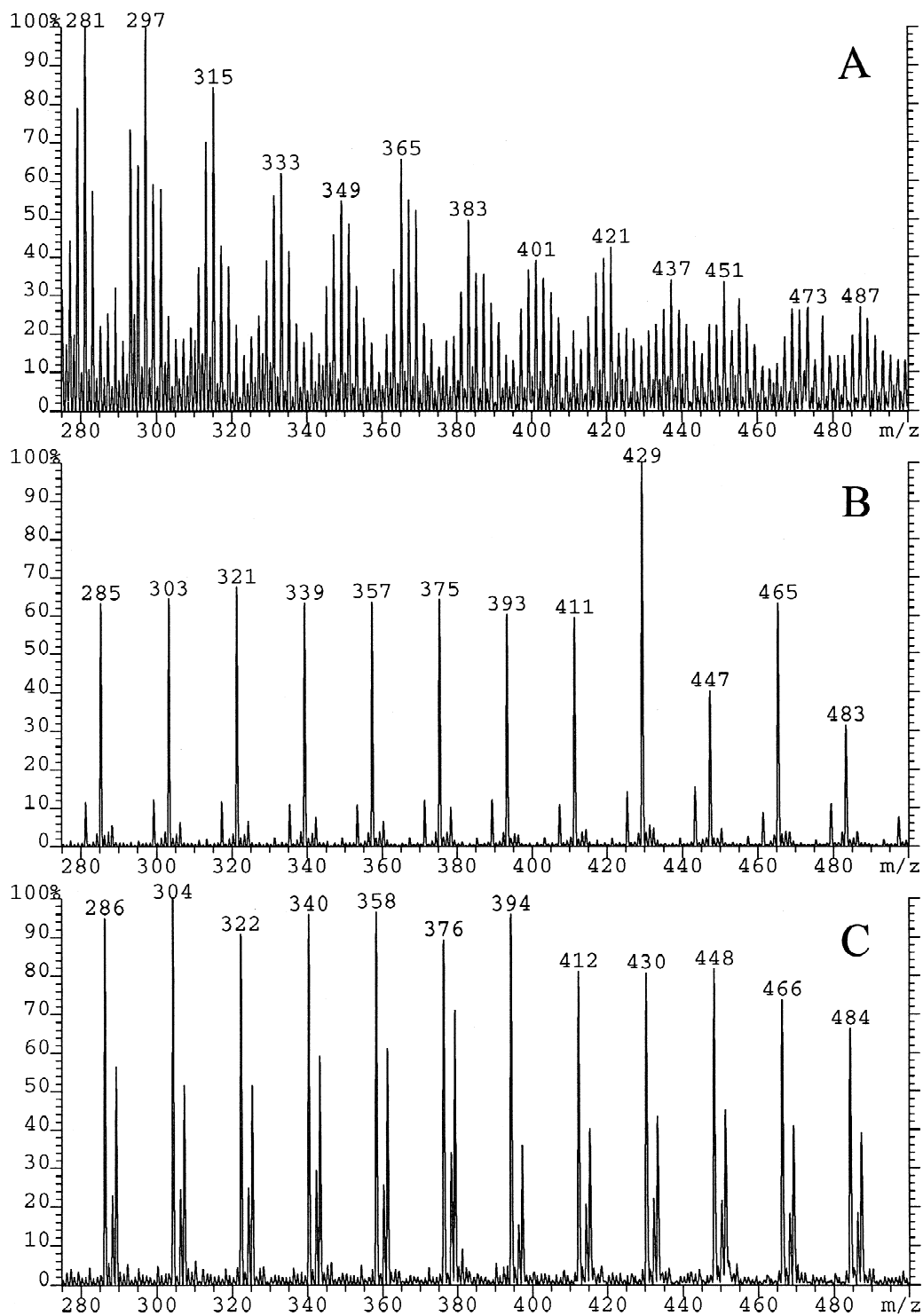
Fig. 6. Selected parts of spectra achieved with water solutions of (A) $H_2O_2$ (3 *M*), (B) $NH_2NH_2$ (65 m*M*), and (C) $NH_2OH$ (10 m*M*).
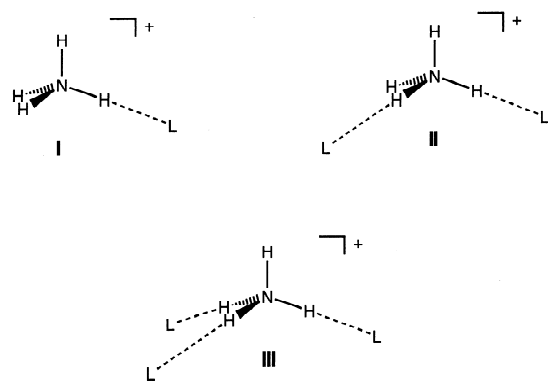
Fig. 7. Cluster ions containing one central ammonium ion and 1–3 ammonia or water ligands L.

or ammonia molecules then the preference for ammonia is lost. This is seen in Fig. 5 since the percentage content of ammonia in the clusters decreases. Most likely, the preference of ammonia is to avoid formation of ring- and cage-structures and instead form shell-like structures [36], which should make the ammonia content decline in large cluster ions. The ability of water to form three-dimensional structures should be higher than that of ammonia. With two lone-pairs and two O–H bonds the $H_2O$ molecule is better suited as a building block in three-dimensional structures than ammonia with only one lone-pair and three N–H bonds. As a result, it is not possible to form fused bicyclic clusters $NH_4^+(NH_3)_n$ completely composed of ammonia. This should explain why there is a tendency not to include ammonia in caged cluster ions. Accordingly, the

more three-dimensional the cluster ion the less will the ammonia content be.

With this in mind one can analyze the cluster ions and make general proposals to their structures. As mentioned, the central ammonium ion is first stabilized by 1–3 ammonia molecules. For slightly larger clusters water starts to intermix. The intensity drop for cluster ions with 8–9 heavy atoms, as seen in Fig. 2, should be due to the fact that monocyclic structures have to be formed and these are most likely not much more internally stabilized by hydrogen-bonding than are open and/or smaller structures. We suggest that bicyclic structures can start to form when it is possible to form two fused five-membered rings, i.e. at $m/z = 144$, and tricyclic structures with three fused five-membered rings at $m/z = 180$. Moreover, we consider bicyclic and tricyclic structures containing four-membered rings as too strained to be formed, even though there are recent proposals made that neutral $(H_2O)_{20}$ is composed of five four-membered rings stacked on each other [37].

The similarities in the spectra of $NH_4^+(H_2O)_n$ and $H_3O^+(H_2O)_n$ cluster ions can be utilized to make general statements about structural alternatives to the dodecahedron for the magic number clusters. It is clear that $H_3O^+(H_2O)_{20}$ contains a $H_3O^+$ and not a $H_5O_2^+$ unit since a difference compared to spectra of clusters with $NH_4^+$ would have been observed in the latter situation. Moreover, at high ammonia concentrations the magic cluster is instead $NH_4^+(H_2O)_{20}(NH_3)_2$ (Fig. 4C), and it is possible that this cluster consists of $NH_4^+(H_2O)_{20}$ coordinated

Table 1
Calculated data at B3LYP/6-311+G(d,p) level for $NH_4(OH_2)_m(NH_3)_n^+$ cluster ions[a]

| Cluster ion | Sym. | Coordination energy | Hydrogen bond lengths | |
|---|---|---|---|---|
| | | | N–H(NH$_3$) | O–H(NH$_3$) |
| 1, $NH_4(OH_2)^+$ | $C_1$ | 22.0 | | 1.637 |
| 2, $NH_4(NH_3)^+$ | $C_{3v}$ | 28.3 | 1.549 | |
| 3, $NH_4(OH_2)_2^+$ | $C_2$ | 40.1 | | 1.716 |
| 4, $NH_4(OH_2)(NH_3)^+$ | $C_1$ | 44.6 | 1.759 | 1.694 |
| 5, $NH_4(NH_3)_2^+$ | $C_2$ | 48.5 | 1.751 | |
| 6, $NH_4(OH_2)_3^+$ | $C_3$ | 55.5 | | 1.777 |
| 7, $NH_4(OH_2)_2(NH_3)^+$ | $C_1$ | 58.9 | 1.782 | 1.805; 1.811 |
| 8, $NH_4(OH_2)(NH_3)_2^+$ | $C_1$ | 61.9 | 1.822; 1.818 | 1.834 |
| 9, $NH_4(NH_3)_3^+$ | $C_3$ | 64.7 | 1.852 | |

[a] Energies in kcal/mol, and bond lengths in Å. Coordination energies refer to the energy for the reaction $NH_4^+ + mOH_2 + nNH_3 \rightarrow NH_4(OH_2)_m(NH_3)_n^+$, $m$ and $n = 0–3$.

by two ammonia molecules onto the outer surface. It should be mentioned that clusters $NH_4^+(H_2O)_{20}(NH_3)_3$ and $NH_4^+(H_2O)_{20}(NH_3)_4$ are slightly less abundant than that containing two ammonia molecules. In Fig. 5 it is clearly seen that the magic numbers for clusters with n numbers of $NH_3$ molecules appear at sizes that correspond to $NH_4^+(H_2O)_{20}(NH_3)_n$, i.e. a central clathrate $NH_4^+(H_2O)_{20}$ to which $n$ numbers of $NH_3$ molecules have coordinated. This observation should indicate that there are specific sites to which ammonia can coordinate. On the dodecaheder, there are no such specific sites and it is difficult to understand why and how the four ammonia molecules would add in this case.

Considering a smooth transfer to ice structure it is tempting to make proposals about structures resembling the hexagonal structure of ice. One such proposal is that shown in Fig. 8, i.e. a structure composed of 6-membered rings in boat conformations. An interesting aspect with this structure is that it has specific sites where ammonia can add to form $NH_4^+(H_2O)_{20}(NH_3)_3$ and $NH_4^+(H_2O)_{20}(NH_3)_4$. Since ammonia forms rather long hydrogen bonds it should be easier for ammonia than for water to bridge between two sites of the 6-membered rings. However, the new proposal has merely 28 (or 29) hydrogen bonds, if those to the central hydronium (or ammonium) ion are counted. Since it was shown that the number of hydrogen bonds is central for the stability of the cluster [13,29], one could estimate that this ion is considerably less stable than the dodecahedral structure which has 33 (or 34) hydrogen bonds.

However, the structures suggested from the DFT calculations of Laasonen and Klein did not give hints

about why there is a magic number at 20 [29]. From their study it is not easy to understand why there are difficulties to enlarge the cluster so that an intensity drop is observed between 20 and 21. Accordingly, new ideas are needed. Through this study it should be possible to give some general guidelines to which structures are allowed, and which are not. Moreover, it is likely that a transfer from well-defined smaller cluster ions to the bulk-like clusters would pass species such as that shown in Fig. 8.

## 5. Conclusions and outlook

The following conclusions can be drawn from the present investigation:
1. Only a slight modification of a standard instrumentation for electrospray ionization is used.
2. The method is suited to the study of weakly bonded cluster ions such as e.g. $H_3O^+(H_2O)_n$.
3. It is possible to obtain high resolution and a high signal-to-noise ratio even at high mass ($m/z > 2000$).
4. Liquid samples can be injected, which enables analysis of any ionic solution. Accordingly, weakly bonded clusters containing metal ions could easily be investigated.
5. The method could be useful for calibration purposes. In this case, a weak ammonia solution is injected, both gas flow and heating is shut off and the nebulising gas pressure is increased.
6. The method can be used for determination of isotopic composition of N, H and O in water and ammonia.

Usage of the method was exemplified on $H_3O^+(H_2O)_n$, $NH_4^+(H_2O)_n$ and $NH_4^+(NH_3)_m(H_2O)_n$ clusters ions. From the analysis it is seen that $H_2O$ and $NH_3$ have different abilities to incorporate into caged three-dimensional structures. Furthermore, $H_3O^+(H_2O)_n$ and $NH_4^+(H_2O)_n$ should have similar structures with a central hydronium or ammonium ion.
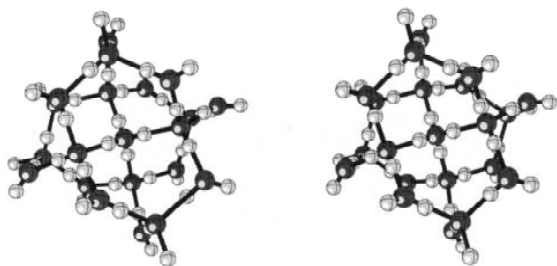
Fig. 8. Stereo view of a proposed structure of the magic number cluster $NH_4^+(H_2O)_{20}$.

## References

[1] J.F. Garvey, W.J. Herron, G. Vaidyanathan, Chem. Rev. 94 (1994) 1999.

[2] A.W. Castleman, R.G. Keesee, Chem. Rev. 86 (1986) 589.

[3] J.Q. Searcy, J.B. Fenn, J. Chem. Phys. 61 (1974) 5282.

[4] J.L. Kassner Jr., D.E. Hagen, J. Chem. Phys. 64 (1976) 1860.

[5] R.J. Beuhler, L. Friedman, J. Chem. Phys. 77 (1982) 2549.

[6] P.M. Holland, A.W. Castleman, J. Chem. Phys. 72 (1980) 5984.

[7] V. Hermann, B.D. Kay, A.W. Castleman, Chem. Phys. 72 (1982) 185.

[8] H. Shinohara, U. Nagashima, H. Tanaka, N. Nishi, J. Chem. Phys. 83 (1985) 4183.

[9] O. Echt, D. Kreisle, M. Knapp, M. Recknagel, Chem. Phys. Lett. 108 (1984) 401.

[10] U. Nagashima, H. Shinohara, N. Nishi, H. Tanaka, J. Chem. Phys. 84 (1986) 209.

[11] S. Wei, Z. Shi, A.W. Castleman, J. Chem. Phys. 94 (1991) 3268.

[12] X. Yang, A.W. Castleman, J. Am. Chem. Soc. 111 (1989) 6845.

[13] T.F. Magnera, D.E. David, J. Michl, Chem. Phys. Lett. 182 (1991) 363.

[14] S. Wei, Z. Shi, A.W. Castleman Jr., J. Chem. Phys. 94 (1991) 3268.

[15] Z. Shi, S. Wei, J.V. Ford, A.W. Castleman, Chem. Phys. Lett. 200 (1992) 142.

[16] Z. Shi, J.W. Ford, S. Wei, A.W. Castleman Jr., J. Chem. Phys. 99 (1993) 8009.

[17] A.P. Tinke, C.E.M. Heeremans, R.A.M. van der Hoeven, W.M.A. Niessen, J. van der Greef, N.M.M. Nibbering, Rapid Commun. Mass Spectrom. 5 (1991) 188.

[18] D.P. Beggs, F.H. Field, J. Am. Chem. Soc. 93 (1971) 1567.

[19] A.J. Cunningham, J.D. Payzant, P. Kebarle, J. Am. Chem. Soc. 94 (1972) 7267.

[20] Y.K. Lau, S. Ikuta, P. Kebarle, J. Am. Chem. Soc. 104 (1982) 1462.

[21] M. Meot-Ner, C.V. Speller, J. Phys. Chem. 90 (1986) 6616.

[22] M. Meot-Ner, F.H. Field, J. Am. Chem. Soc. 99 (1977) 998.

[23] H.A. Schwarz, J. Chem. Phys. 67 (1977) 5525.

[24] L.I. Yeh, M. Okumura, J.D. Myers, J.M. Price, Y.T. Yee, J. Chem. Phys. 91 (1989) 7319.

[25] M.D. Newton, J. Chem. Phys. 67 (1978) 5535.

[26] D. Wei, D.R. Salahub, J. Chem. Phys. 101 (1994) 7633.

[27] J.M. Seminario, P. Politzer (Eds.), Modern Density Functional Theory: A Tool for Chemistry, Elsevier, Amsterdam, 1995.

[28] A. Khan, Chem. Phys. Lett. 217 (1994) 443.

[29] K. Laasonen, M.L. Klein, J. Phys. Chem. 98 (1994) 10079.

[30] E.M. Evleth, Z.D. Hamon-Tahra, E. Kassab, J. Phys. Chem. 95 (1991) 1213.

[31] M.J. Frisch, J.E. Del Bene, J.S. Binkley, H.F. Schaefer III, J. Chem. Phys. 84 (1986) 2279.

[32] A.D. Becke, J. Chem. Phys. 98 (1993) 5648.

[33] P.J. Stevens, F.J. Devlin, C.F. Chablowski, M.J. Frisch, J. Phys. Chem. 98 (1994) 11623.

[34] M.J. Frisch, G.W. Trucks, H.B. Schlegel, P.W.M. Gill, B.G. Johnson, M.A. Robb, J.R. Cheeseman, T. Keith, G.A. Petersson, J.A. Montgomery, K. Raghavachari, M.A. Al-Laham, V.G. Zakrzewski, J.V. Ortiz, J.B. Foresman, J. Cioslowski, B.B. Stefanov, A. Nanayakkara, M. Challacombe, C.Y. Peng, P.Y. Ayala, W. Chen, M.V. Wong, J.L. Andres, R.S. Repogle, R. Gomperts, R.L. Martin, D.J. Fox, J.S. Binkley, D.J. Defrees, J. Baker, J.P. Stewart, M. Head-Gordin, C. Gonzales, J.A. Pople, Gaussian 94, Rev. C.3, Gaussian Inc., Pittsburgh, PA, 1995.

[35] W. Jensen, J. Chem. Rev. 78 (1978) 1.

[36] M. Ichihashi, J. Yamabe, K. Murai, S. Nonose, K. Hirao, T. Kondow, J. Phys. Chem. 100 (1996) 10050.

[37] C. Lee, H. Chen, G. Fitzgerald, J. Phys. Chem. 102 (1995) 1266.